

Biophysical Journal, Volume 114

Supplemental Information

**Mathematical Models for Cell Migration with Real-Time Cell Cycle
Dynamics**

Sean T. Vittadello, Scott W. McCue, Gency Gunasingh, Nikolas K. Haass, and Matthew J. Simpson

Contents

1	Numerical solutions of the mathematical model	2
2	Scratch assay of FUCCI-transduced WM983C melanoma cells	3
3	Numerical solutions demonstrating travelling wave behaviour	5
	References	6

1 Numerical solutions of the mathematical model

The numerical solutions of Eqs (2)–(3) and Eqs (4)–(6) are obtained using an implicit finite difference approximation. In particular, we use a central difference approximation for the spatial derivative term, and a backward Euler approximation for the temporal derivative [1]. The spatial domain, $0 \leq x \leq L$, is uniformly discretised with grid spacing Δx . No-flux boundary conditions are implemented at both $x = 0$ and $x = L$. The temporal domain is uniformly discretised with time steps of duration Δt . The resulting non-linear system of equations is solved using the Thomas algorithm [1], applying Picard iteration at each time step until the maximum absolute change in the given dependent variable across the spatial grid is less than a specified tolerance, ϵ .

2 Comparison of experimental data and the fundamental model for a scratch assay of FUCCI-transduced WM983C melanoma cells.

In Fig S1 we present experimental data for the WM983C melanoma cell line, together with corresponding numerical solutions of the fundamental model. The numerical solutions compare well with the experimental data.

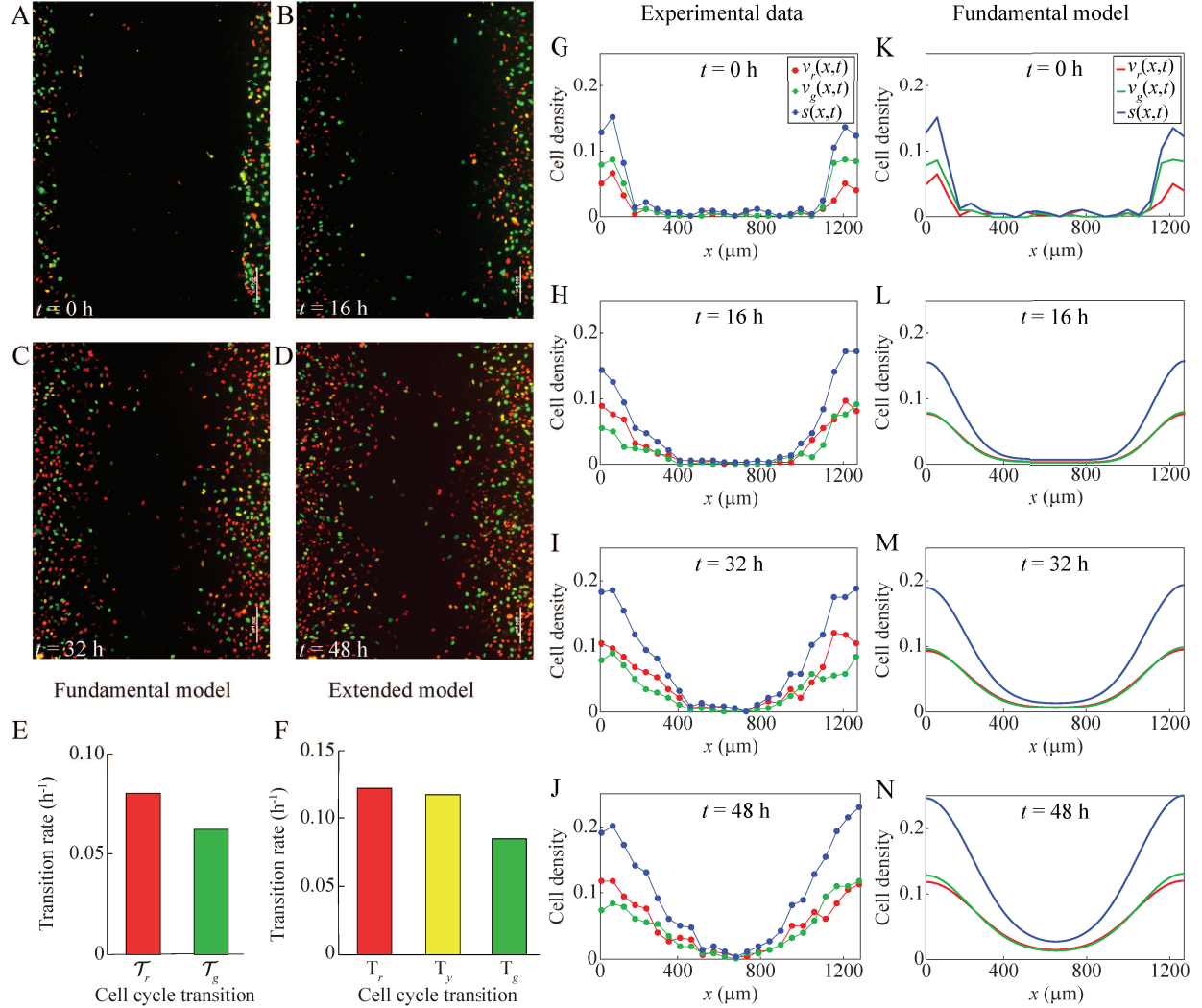


Figure S1: Comparison of experimental data and the fundamental model for a scratch assay of FUCCI-transduced WM983C melanoma cells. (A)–(D) Still images of a scratch assay with FUCCI-transduced WM983C melanoma cells at time 0 h, 16 h, 32 h and 48 h, respectively. Scale bar is $200 \mu\text{m}$. (E) Estimated transition rates from one cell cycle phase to the next for the fundamental model with two subpopulations, based on data from the WM983C cell line from Fig 1C in [2]. (F) Estimated transition rates from one cell cycle phase to the next for the extended model with three subpopulations, based on data from the WM983C cell line from Fig 1C in [2]. (G)–(J) Experimental non-dimensional cell density data at 0 h, 16 h, 32 h and 48 h, respectively (based on images (A)–(D)). The cell density is treated as a function of x and t only, owing to the fact that the initial density does not depend on the vertical coordinate, y . (K)–(N) Numerical solutions of the fundamental model, Eqs (2)–(3), at 0 h, 16 h, 32 h and 48 h. The numerical solutions are obtained with $\Delta x = 0.1 \mu\text{m}$, $\Delta t = 0.1 \text{h}$, $L = 1254 \mu\text{m}$, diffusion coefficients $\mathcal{D}_r = \mathcal{D}_g = 400 \mu\text{m}^2 \text{h}^{-1}$, transition rates $\kappa_r = 0.080 \text{h}^{-1}$ and $\kappa_g = 0.062 \text{h}^{-1}$, and initial conditions the same as for the experimental data.

3 Numerical solutions demonstrating travelling wave behaviour for the fundamental model when $\mathcal{D} \neq 1$.

In Fig S2 we present numerical solutions of the fundamental model, Eqs (2)–(3), with $\mathcal{D} \neq 1$. In Fig S2A, $\mathcal{D} = 0.5$, and in Fig S2B, $\mathcal{D} = 2$. These solutions are qualitatively the same as for $\mathcal{D} = 1$, see Fig 3, demonstrating that the existence of these travelling waves is robust, and does not depend on the value of $\mathcal{D}_g/\mathcal{D}_r$.

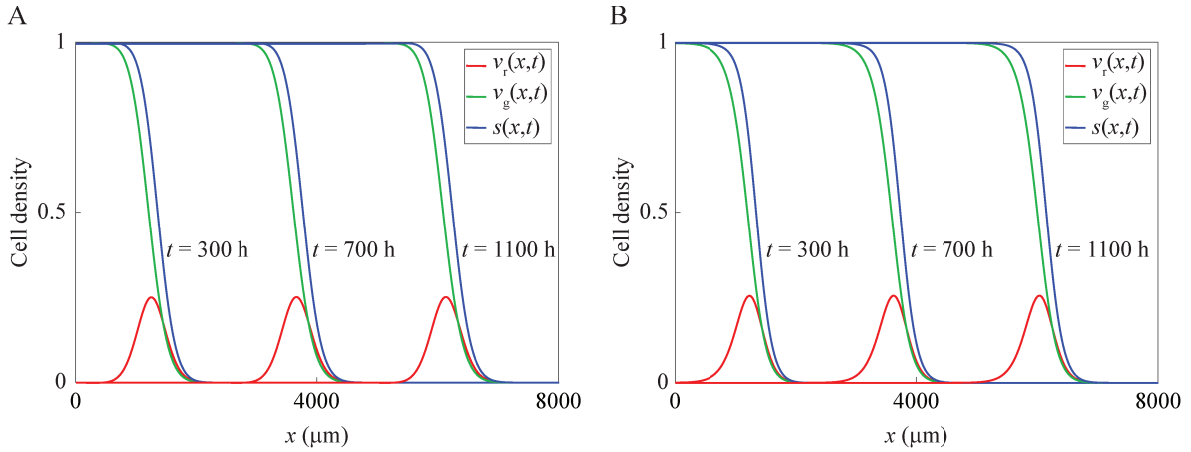


Figure S2: Numerical solutions of the fundamental model, Eqs (2)–(3), demonstrating travelling wave behaviour with $\mathcal{D} \neq 1$. (A) Solutions obtained with $\Delta x = 0.1 \mu\text{m}$, $\Delta t = 0.1 \text{ h}$, $L = 8000 \mu\text{m}$, $\mathcal{D}_r = 400 \mu\text{m}^2 \text{ h}^{-1}$, $\mathcal{D}_g = 200 \mu\text{m}^2 \text{ h}^{-1}$, $\kappa_r = \kappa_g = 0.08 \text{ h}^{-1}$, and the initial condition given by Eq (9) with $\xi = 10$. (B) Solutions obtained with $\Delta x = 0.1 \mu\text{m}$, $\Delta t = 0.1 \text{ h}$, $L = 8000 \mu\text{m}$, $\mathcal{D}_r = 200 \mu\text{m}^2 \text{ h}^{-1}$, $\mathcal{D}_g = 400 \mu\text{m}^2 \text{ h}^{-1}$, $\kappa_r = \kappa_g = 0.08 \text{ h}^{-1}$, and the initial condition given by Eq (9) with $\xi = 10$.

References

- [1] Morton, K. W. and D. F. Mayers, 2005. Numerical Solution of Partial Differential Equations. 2nd ed. Cambridge: Cambridge University Press.
- [2] Haass, N. K., K. A. Beaumont, D. S. Hill, A. Anfosso, P. Mrass, M. A. Munoz, I. Kinjyo, and W. Weninger, 2014. Real-time cell cycle imaging during melanoma growth, invasion, and drug response. *Pigment Cell Melanoma Res.* 27:764–776.